

Cluster-induced crater formation

Christian Anders, Gerolf Ziegenhain, Steffen Zimmermann, and Herbert M. Urbassek*

*Fachbereich Physik, Universität Kaiserslautern,
Erwin-Schrödinger-Straße, D-67663 Kaiserslautern, Germany*

(Dated: November 1, 2018)

Abstract

Using molecular-dynamics simulation, we study the crater volumes induced by energetic impacts ($v = 1 - 250$ km/s) of projectiles containing up to $N = 1000$ atoms. We find that for Lennard-Jones bonded material the crater volume depends solely on the total impact energy E . Above a threshold E_{th} , the volume rises linearly with E . Similar results are obtained for metallic materials. By scaling the impact energy E to the target cohesive energy U , the crater volumes become independent of the target material. To a first approximation, the crater volume increases in proportion with the available scaled energy, $V = aE/U$. The proportionality factor a is termed the cratering efficiency and assumes values of around 0.5.

PACS numbers: 79.20.Ap, 61.80.Az, 61.80.Lj, 79.20.Rf

arXiv:0810.4242v1 [cond-mat.mtrl-sci] 23 Oct 2008

I. INTRODUCTION

The erosion of surfaces by atom or ion impact – i.e., the sputter process – has for long been studied.^{1–4} More recently, interest has focussed on erosion by cluster impact both experimentally^{5–9} and by computer simulations.^{10–16} We shall investigate in this paper the question how the crater volume depends on the cluster energy and cluster size N and, – more specifically – whether it is the total energy E of the cluster, or rather the energy per atom E/N , which is decisive to determine the cluster volume. We shall employ two widely differing classes of materials to study this question, a van-der-Waals bonded target, and metals, in order to show in how far our considerations are materials independent.

II. METHOD

We employ the method of molecular-dynamics simulation to shed light on the process of crater formation. This technique is standard, and will not be presented here. Details are given elsewhere.^{13,17–20} In short: The clusters are chosen of a spherical shape and consist of $1 \leq N \leq 1000$ atoms. For the Ar system, a Lennard-Jones potential,^{21,22} and for the Cu and Au targets a many-body potential of the embedded-atom type²³ has been chosen.^{12,16,24} In all cases, the potentials have been splined to an appropriate high-energy potential^{25,26} in order to accurately model close collisions. The size of the target system varies between 7×10^4 and approximately 7×10^6 atoms, depending on the total cluster energy E . At the lateral and bottom sides of the simulation target, we employ damped boundary conditions in order to mimic energy dissipation to the surrounding target material. The Cu target consists of an fcc crystal with (100) surface; for the Au crystal a (111) surface has been chosen. In the case of Ar, we employ an amorphous target. We determine temperature and pressure in our simulation as local quantities, which are averaged over a sphere with a radius equal to the cutoff radius of the potential (containing around 50 atoms) to reduce fluctuations.²⁷

III. RESULTS

Fig. 1 displays the results of Ar₁₀₀₀ impact on an amorphous Ar surface at 4 keV impact energy. A compression wave moves hemispherically out of the impact point. The material

within the immediate impact zone is seen to have gasified; this process still continues at the time of $t = 3$ ps, where the snapshots are displayed. Note that the temperatures in the central region are high, far above the melting and even the boiling point of this material. The latest snapshot shown ($t = 60$ ps) demonstrates that the crater has considerably widened. The relatively high temperatures present indicate that the crater form will still relax to some degree after this time. The simulation results show that the sputtering process corresponds to a *phase explosion*, in which sputtering occurs by the gasification of the high-energy-density zone, as long as this is situated sufficiently close to the surface.

The impact of a Cu_{1000} cluster on a Cu target is displayed in Fig. 2. Here the crater formation is a faster process, and hence we display atomistic snapshots already at time of $t = 1$ ps. Temperatures do not reach so high values, when compared to typical materials parameters such as the triple or critical temperature; the crater walls are molten, but the boiling point is not reached. However, the pressure reaches high values: Immediately below the crater, a zone of high compressive pressure has formed; its anisotropy reflects the crystallinity of the target. Close to the surface, we observe already a zone of tensile pressure forming; the further evolution of this zone will be discussed elsewhere. At the final time displayed, the form of the crater seems to have stabilized; the temperature is close to zero. Note that the crater has apparently shrunk after $t = 1$ ps in the course of the target relaxation.

We define the crater volume as the ensemble of missing atoms below the original surface. Consequently, we measure the crater volume V as a dimensionless quantity, viz., the equivalent number of missing target atoms. The total kinetic energy of the impacting cluster, E , will be scaled to the target cohesive energy, U , and is thus measured as a dimensionless energy

$$\epsilon = E/U. \tag{1}$$

For the materials used in our study, it is $U = 0.0815$ (3.54, 3.79) eV for Ar (Cu, Au). Fig. 3 summarizes the energy dependence of the crater volumes induced in the two materials studied. Analogous results for smaller cluster size $N = 100$ have been published previously.²⁸ In both cases, self-bombardment by clusters containing 1000 atoms has been simulated. Evidently the crater volumes for these two widely different materials coincide rather well when the impact energy is scaled to the target cohesive energy, $\epsilon = E/U$. The data are –

to a good first approximation – well described by a linear law

$$V = a(\epsilon - \epsilon_c), \quad \epsilon > \epsilon_c, \quad (2)$$

where the *cratering efficiency* $a \cong 0.5$, Ar (Cu), and the threshold energy is $\epsilon_c \cong 4700$. More precisely, a linear fit to our data gives $a = 0.52 \pm 0.02$ and $\epsilon_c = 4725 \pm 480$ for Ar, while the fit for Cu yields $a = 0.47 \pm 0.04$ and $\epsilon_c = 4725 \pm 1570$.

We rationalize the simple law, Eq. (2), in which only one materials parameter, the cohesive energy U , describes the physics, as follows: The cluster is quickly stopped in the target, on a time scale $t_0 \cong d/v$, where d is the cluster diameter, and v its impact velocity.²⁹ After this time, virtually all the cluster energy E is available close to the target surface for crater formation. The available energy can then be used for bond breaking in the target and hence atomize the material in the energized region, which is to become the crater volume.

Finally, Fig. 4 assembles the simulated crater sizes from the present simulations and combined with a larger set of previous simulations on small Cu clusters ($N = 13, 43$).¹⁷ Data for Au cluster impacts are also shown, which have been extracted from our previous simulations.^{16,30} These latter data are fitted to a law

$$V = c \frac{\epsilon^{1+d}}{(\epsilon + \epsilon_c)^d}, \quad (3)$$

with $c = 0.511$, $\epsilon_c = 1320$, and $d = 1.5$. Such a law may be better suited to describe the threshold behaviour, while for large ϵ , it again leads to a linear increase.¹⁹ Fig. 4 demonstrates that in the energy regime studied here, the linear regime describes well crater volumes both in condensed noble gases and metal target. The threshold regime, however, is dependent on materials and, in particular, on the cluster size.

In Fig. 5, we plot the same data as a function of the energy per particle, E/N . Note that for a fully linear volume-energy relationship, with size independent parameters, again all data should converge to one universal line. We see that for high impact velocities, $\epsilon/N \gtrsim 100$, this is indeed the case. In the threshold regime, however, the data show an increasingly strong dependence on cluster size.

IV. CONCLUSION

1. Molecular-dynamics simulations of cluster-induced crater volumes V give comparable results for different target materials if the cluster energy E is scaled to the target cohesive energy U .
2. Above a threshold E_{th} , the crater volume V increases linearly with the cluster energy E .
3. Crater formation sets in when the excitation strength exceeds a certain threshold. This threshold is mainly characterized by an energy criterion, such that the cluster impact energy scaled to the cohesive energy of the target must exceed a threshold value, which is only mildly dependent on the material. These thresholds attain similar values, even for so drastically different materials as van-der-Waals bonded materials and metals.

* Electronic address: `urbassek@rhrk.uni-kl.de`; URL: `http://www.physik.uni-kl.de/urbassek/`

¹ R. Behrisch, ed., *Sputtering by particle bombardment I* (Springer, Berlin, 1981).

² R. Behrisch, ed., *Sputtering by particle bombardment II* (Springer, Berlin, 1983).

³ R. Behrisch and K. Wittmaack, eds., *Sputtering by particle bombardment III* (Springer, Berlin, 1991).

⁴ R. Behrisch and W. Eckstein, eds., *Sputtering by Particle Bombardment*, vol. 110 of *Topics Appl. Physics* (Springer, Berlin, 2007).

⁵ H. H. Andersen, A. Brunelle, S. Della-Negra, J. Depauw, D. Jacquet, and Y. LeBeyec, *Phys. Rev. Lett.* **80**, 5433 (1998).

⁶ A. Brunelle, S. Della-Negra, J. Depauw, D. Jacquet, Y. LeBeyec, M. Pautrat, K. Baudin, and H. H. Andersen, *Phys. Rev. A* **63**, 022902 (2001).

⁷ S. Bouneau, A. Brunelle, S. Della-Negra, J. Depauw, D. Jacquet, Y. LeBeyec, M. Pautrat, M. Fallavier, J. C. Poizat, and H. H. Andersen, *Phys. Rev. B* **65**, 144106 (2002).

⁸ H. H. Andersen, A. Johansen, M. Olsen, and V. Touboltsev, **212**, 56 (2003).

- ⁹ A. Brunelle and S. Della-Negra, **222**, 68 (2004).
- ¹⁰ Z. Insepov and I. Yamada, **153**, 199 (1999).
- ¹¹ M. H. Shapiro and T. A. Tombrello, **217**, 253 (2004).
- ¹² T. J. Colla and H. M. Urbassek, **164-165**, 687 (2000).
- ¹³ T. J. Colla, R. Aderjan, R. Kissel, and H. M. Urbassek, Phys. Rev. B **62**, 8487 (2000).
- ¹⁴ Y. Yamaguchi and J. Gspann, Phys. Rev. B **66**, 155408 (2002).
- ¹⁵ E. Salonen, K. Nordlund, and J. Keinonen, **212**, 286 (2003).
- ¹⁶ S. Zimmermann and H. M. Urbassek, **228**, 75 (2005).
- ¹⁷ R. Aderjan and H. M. Urbassek, **164-165**, 697 (2000).
- ¹⁸ C. Schäfer, H. M. Urbassek, and L. V. Zhigilei, Phys. Rev. B **66**, 115404 (2002).
- ¹⁹ C. Anders, H. M. Urbassek, and R. E. Johnson, Phys. Rev. B **70**, 155404 (2004).
- ²⁰ A. K. Upadhyay and H. M. Urbassek, Phys. Rev. B **73**, 035421 (2006).
- ²¹ A. Michels, H. Wijker, and H. K. Wijker, **15**, 627 (1949).
- ²² J.-P. Hansen and L. Verlet, Phys. Rev. **184**, 151 (1969).
- ²³ M. S. Daw, S. M. Foiles, and M. Baskes, **9**, 251 (1993).
- ²⁴ Y. Mishin, D. Farkas, M. J. Mehl, and D. A. Papaconstantopoulos, Phys. Rev. B **59**, 3393 (1999).
- ²⁵ W. D. Wilson, L. G. Haggmark, and J. P. Biersack, Phys. Rev. B **15**, 2458 (1977).
- ²⁶ J. F. Ziegler, J. P. Biersack, and U. Littmark, *The Stopping and Range of Ions in Solids* (Pergamon, New York, 1985).
- ²⁷ T. J. Colla and H. M. Urbassek, **142**, 439 (1997).
- ²⁸ H. M. Urbassek, C. Anders, L. Sandoval, and A. K. Upadhyay, in *High-Power Laser Ablation VII*, edited by C. R. Phipps (2008), vol. 7005 of *Proc. SPIE*, pp. 700507-1 – 12.
- ²⁹ C. Anders and H. M. Urbassek, **258**, 497 (2007).
- ³⁰ S. Zimmermann and H. M. Urbassek, **255**, 208 (2007).

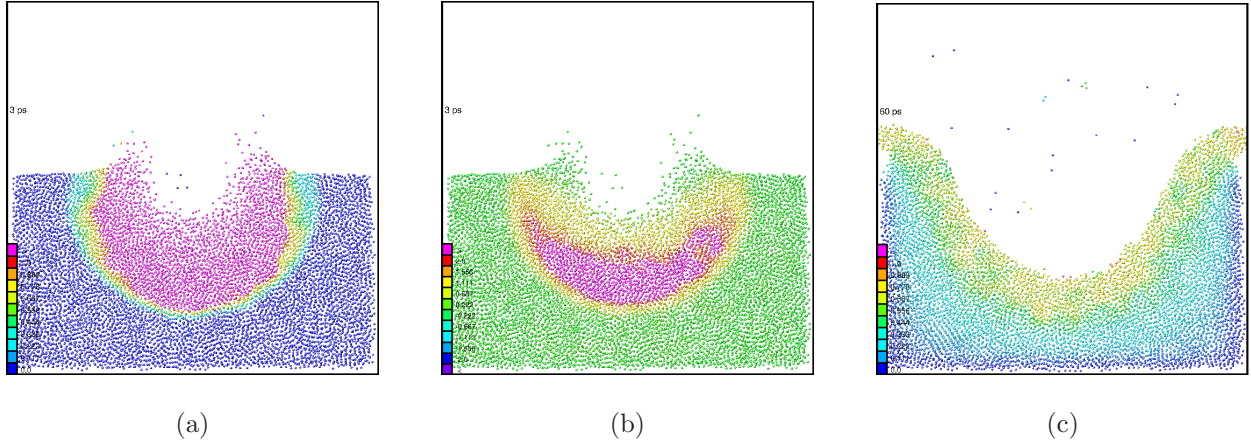


FIG. 1: Snapshots of $\text{Ar}_{1000} \rightarrow \text{Ar}$ impact at an impact energy of $E = 4$ keV, $\epsilon \cong 49,000$. a: Temperature distribution in the target at $t = 3$ ps after cluster impact. Color denotes temperature in units of the boiling temperature of Ar (87.3 K). b: Pressure distribution in the target at $t = 3$ ps after impact. Color: pressure in units of GPa. Green denotes zero pressure, while the highest pressure (purple) is compressive at > 2 GPa. c: Crater formed at $t = 60$ ps after impact. Color denotes temperature as in subfigure (a).

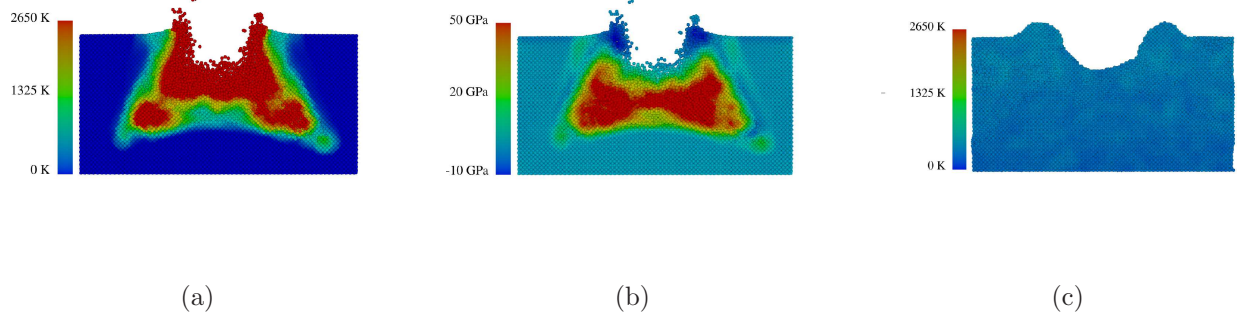


FIG. 2: Molecular-dynamics view of crater formation in a Cu target bombarded by a Cu_{1000} projectile at $E = 50,000$ eV, $\epsilon \cong 14,100$. a: Temperature distribution in the target at $t = 1$ ps after cluster impact. b: Pressure distribution in the target at $t = 1$ ps after impact. Turquoise denotes zero pressure, positive pressure is compressive, while negative pressure is tensile. c: Crater formed at $t = 50$ ps after impact.

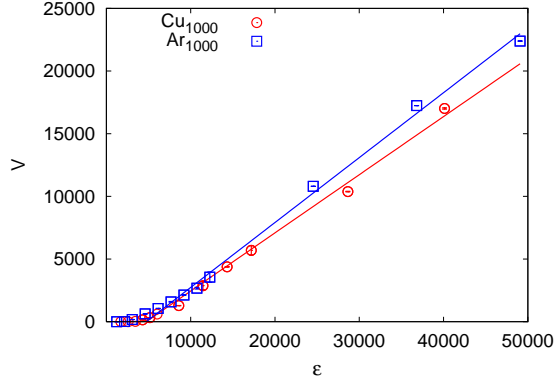


FIG. 3: Dependence of the cluster volume V on the scaled impact energy, $\epsilon = E/U$. Self-bombardment of clusters containing $N = 1000$ atoms on Ar and Cu has been simulated.

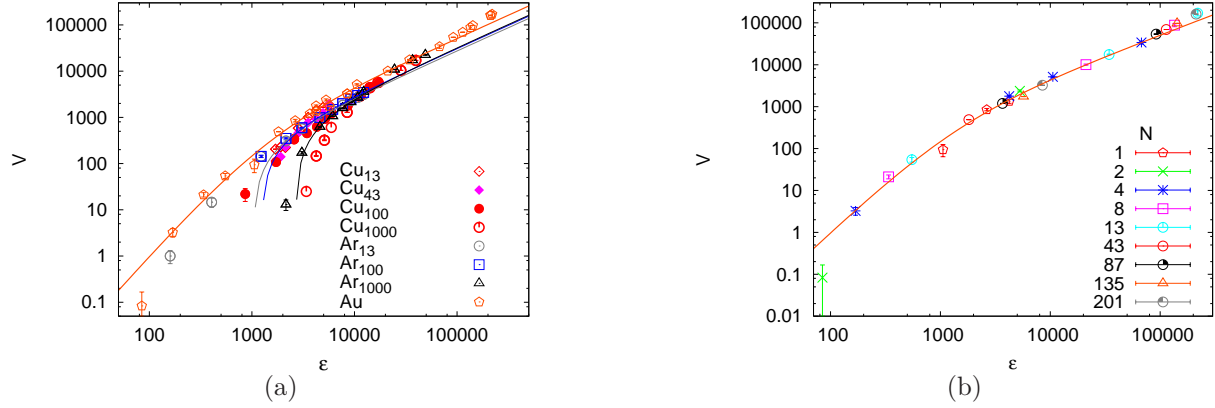


FIG. 4: Synopsis of simulational data of crater volumes V vs scaled energies $\epsilon = E/U$. Data for small Cu clusters ($N = 13, 43$) taken from Ref. 17. Legend indicates projectiles. Lines indicate (asymptotically) linear relationships, Eqs. (2) and (3). Lines in subfigures (a) and (b) are identical. (b) details the energy and size dependence of the Au data of subfigure (a).

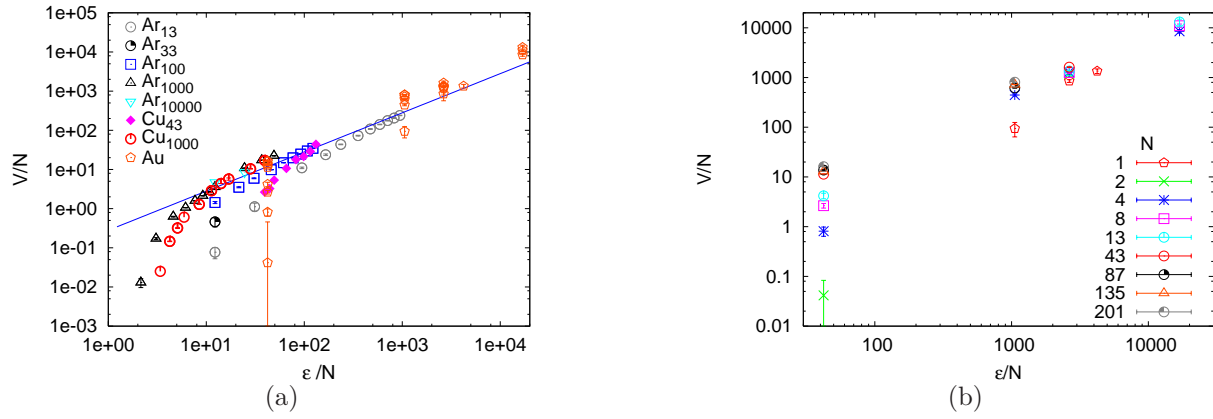


FIG. 5: Data of Fig. 4 scaled to cluster size N . Legend indicates projectiles. Lines indicate a linear relationship. Lines identical to those in Fig. 4.